Improved Joint Zero Offset Calibration for Industrial Cobot Arms

Dante Neckmar

LUND
UNIVERSITY

Department of Automatic Control

MSc Thesis
TFRT-6311
ISSN 0280-5316

Department of Automatic Control
Lund University
Box 118
SE-221 00 LUND
Sweden

© 2026 Dante Neckmar. All rights reserved.
Printed in Sweden by Tryckeriet i E-huset
Lund 2026

Abstract

Collaborative robots, or cobots, are increasingly used in industrial automation, where they work in flexible, semi-modular configurations while still being expected to meet demanding positioning accuracy requirements. After a joint is replaced on such a robot, the resulting joint zero offset typically forces a full kinematic recalibration before the robot can return to service, causing downtime and requiring specialized equipment. Existing solutions are either simple manual references that lack the accuracy needed, or external optical systems that are expensive and complex to set up. This thesis develops a low-complexity, joint-level zeroing method for the cobot arms produced by Kassow Robots, with the goal of avoiding that recalibration step.

A sensitivity analysis showed that a pin-level repeatability of around 20μm is sufficient to keep the tool center point (TCP) positioning error below 1 mm across the full product range. Three concepts were considered: a mechanical fixture, a laser triangulation system, and a vision-based solution. The mechanical concept was chosen for its lower complexity and cost, and was designed and built as a cup-shaped fixture with a self-locking block that engages the joint output through well-defined contact.

A 3D-printed prototype was used to validate the principle, and a machined stainless steel version was then tested over 96 zeroing cycles. The proposed prototype achieved a TCP standard deviation of 0.18 mm and a joint reference pin-level repeatability of about 3μm, well within the requirement. The results show that a passive mechanical fixture can deliver the precision needed for joint replacement without optical hardware or firmware modifications, removing the need for full kinematic recalibration after joint maintenance.

Acknowledgments

First, I would like to thank my supervisor at Lund University, Yiannis Karayiannidis, for his guidance, feedback, and patience throughout this thesis. His comments shaped both the structure and the technical depth of the work.

I am equally grateful to Nicholas Jones at Kassow Robots for the day-to-day support, the many discussions, and the willingness to share both expertise and time in the office. The project would not have been possible without his involvement.

Thank you to Kassow Robots and Kristian Kassow for hosting this thesis, providing the hardware, the expertise, and giving me access to a real industrial setting in which to develop and test the work.

I would also like to thank Lund University and the Department of Automatic Control for the education that made this thesis possible.

Finally, a heartfelt thank you to my life partner Linn and to my parents, for their support, patience, and encouragement throughout this period. None of this would have been the same without you.

Dante Neckmar, Lund, 2026

Contents

1. Introduction **9**
- 1.1 Background . . . 9
- 1.2 Problem Description . . . 10
- 1.3 Research Questions . . . 10
- 1.4 Scope and Delimitations . . . 11
- 1.5 Thesis Structure . . . 11

2. Previous Work **13**
- 2.1 Zeroing methods . . . 13
- 2.2 Broader Calibration Approaches . . . 14
- 2.3 Summary . . . 15

3. Theoretical Background **16**
- 3.1 Robot Kinematics and Error Propagation . . . 16
- 3.2 Forward Kinematics . . . 17
- 3.3 Joint Zero Offset and Absolute Positioning Accuracy . . . 17
- 3.4 Absolute Accuracy and Repeatability . . . 18
- 3.5 Mechanical Precision and Structural Considerations . . . 18
- 3.6 Measurement Resolution . . . 18

4. System design **19**
- 4.1 Requirements Analysis . . . 19
- 4.2 Concept Generation and Selection . . . 22
- 4.3 Detailed Design and Prototyping . . . 26
- 4.4 Future Improvements . . . 29

5. Testing **31**
- 5.1 Experimental Setup . . . 31
- 5.2 Test Procedure . . . 31
- 5.3 Repeatability Test . . . 32
- 5.4 Reproducibility Test . . . 32

6. Results **34**

7. Discussion **38**
7.1 Performance Against the TCP Requirement 38
7.2 Outlier Analysis 38
7.3 Comparison Between Prototype Iterations 39
7.4 Comparison with Previous Work 40
7.5 Implications for Manufacturing Tolerances and Cost 40
7.6 Limitations of the Study 41
8. Conclusion **42**
Bibliography **44**

1

Introduction

1.1 Background

The use of industrial robots and cobots has increased significantly over recent decades due to their flexibility and ability to meet high productivity demands in applications such as welding, painting, assembly, and packaging operations[Toquica and Motta, 2022].

Many manufacturing processes involve tight tolerances between components, which necessitate high positional accuracy. Positioning errors on the order of fractions of a millimeter can lead to increased wear or damage to the parts involved. Consequently, positional accuracy is a key performance indicator in such applications. In flexible industrial assembly systems, robots experience abrasive wear of transmission components, such as ball bearings, as a consequence of operating under very tight tolerances. Over time, this wear can require maintenance or repair actions, which may alter the robot's mechanical properties and lead to deviations from the nominal kinematic model. In order to restore positioning accuracy, a recalibration of the robot is therefore necessary.[Kana et al., 2022] Although various calibration methodologies exist, they generally require external measurement systems, controlled environments, and specialized procedures.

The absolute positioning accuracy of industrial robots depends on how accurately the robot joints are zeroed. The accuracy is affected by many individual factors such as link parameter errors, temperature, wear, and maintenance[Elatta et al., 2004]. One significant contributor to absolute positioning error is the joint zero offset, defined as the deviation between the encoder defined electrical zero and the mechanical reference position assumed in the robot's kinematic model. Even small angular zero offsets propagate through the serial kinematic chain and may result in millimeter level errors at tool center point (TCP), particularly for the base joints with long effective lever arms. According to [Gao et al., 2014], joint zero offset errors can amount to up to 90% of the TCP error. This issue becomes especially relevant in semi-modular robot architectures where individual joints can be replaced independently during maintenance. In such systems, the ability to accurately establish or re-establish the joint zero position, referred to in the future as joint zeroing,

without performing a complete kinematic recalibration is of substantial importance, both monetarily and time-efficiently.

The experiment described in this thesis was conducted on robots from Kassow Robots. Kassow Robots is a young robotics company founded in 2015 in Copenhagen by Kristian Kassow, who also co-founded Universal Robots. The business plan was to develop 7-axes cobots for industrial use. The robots are developed with focus on light weight, high payload per unit footprint, and flexibility.[1] Joint zeroing is the process of rotationally aligning defined mechanical features on the housing and output of a robot joint. The resulting alignment establishes the reference point corresponding to zero rotation, which is then stored in the firmware of the specific joint. Once embedded, the zero position defines how the encoder readings are interpreted within the robot's kinematic model.

1.2 Problem Description

At Kassow Robots, current assembly and maintenance procedures achieve a level of joint zeroing accuracy that is sufficient for general assembly and operation. However, after joint replacement, the resulting absolute positioning error at the robot tool flange may reach several millimeters prior to full robot recalibration. While this deviation can later be corrected through a comprehensive calibration procedure, the process introduces downtime, cost, and requires a sensitive calibration system.

The motivation of this thesis is therefore to research and develop a high-precision joint level zeroing system that enables joint replacement without requiring full robot recalibration. This will include ideation, feasibility analysis, and development of a zeroing rig, with focus on efficiency, robustness, accuracy, precision and cost-efficiency.

Preliminary sensitivity calculations performed during the start of this project indicate that achieving a TCP accuracy of approximately $\pm$1mm, for larger robot configurations, would require a mechanical zeroing repeatability on the order of $\pm 20\mu$m at the reference pin.

1.3 Research Questions

The overall objective of this thesis is to research, develop and validate a high-precision joint zeroing system that is significantly more accurate than the current method and that is feasible for use in an industrial production or service environment to reduce downtime and improve production throughput after maintenance of joints. The problems in question that will be researched are the following:

- What joint zeroing repeatability at the reference pin is required to achieve a TCP positioning error below 1mm across all robot configurations?

[1] Public information about Kassow Robots retrieved from: https://www.kassowrobots.com/about-us

- Which zeroing concepts are technically capable of meeting the accuracy requirement, and what are their trade-offs in cost, robustness, and industrial feasibility?
- How can the selected solution be integrated with existing joint firmware and calibration interfaces?
- Does the developed prototype demonstrate sufficient repeatability and robustness to justify industrial implementation?

1.4 Scope and Delimitations

This thesis focuses on the development and validation of a high-precision joint zeroing method for industrial robot joints, with the primary objective of reducing or eliminating the need for full robot recalibration after joint replacement. This will include: definition of quantitative accuracy requirements, concept generation and feasibility analysis of alternative zeroing approaches, mechanical and/or sensor-based design development, prototype manufacturing for at least one joint size, integration with existing joint control and firmware interfaces, and validation of repeatability and accuracy. The system is designed for use in an industrial production or service environment and must consider cost, robustness, and usability in addition to accuracy.

To maintain a manageable and well defined project scope, several delimitations are imposed. Since the primary objective is to improve joint-level zeroing accuracy, the study focuses exclusively on joint zero offset error and does not redesign or replace the full kinematic calibration procedure. Only the largest joint size, situated in the base joint and the shoulder joint of the largest robot configuration, is prototyped and validated, as this represents the most demanding case in terms of required accuracy. Long-term wear effects and life cycle durability of the final design are outside the scope of this work. Finally, full-robot testing is limited to a subset of configurations as comprehensive multi-joint validation goes beyond what is necessary to demonstrate the core concept.

1.5 Thesis Structure

The remainder of this thesis is organized as follows. Chapter 2 reviews previous work on joint zeroing and robot calibration, covering service mastering procedures, optical joint-offset estimation, and full kinematic recalibration, and positions the present work relative to these approaches. Chapter 3 presents the theoretical background, including robot kinematics, forward kinematics, and the way joint zero offsets propagate through the serial kinematic chain to produce errors at the TCP. Chapter 4 describes the system design, beginning with the requirements analysis

and sensitivity study that establish the required pin-level repeatability followed by the generation and selection of candidate concepts and the detailed design and prototyping of the chosen mechanical fixture. Chapter 5 details the experimental setup and test procedure used to evaluate repeatability. Chapter 6 presents the results from both the 3D-printed prototype and the machined metal fixture, together with a short cost analysis. Chapter 7 discusses these results in relation to the TCP requirement, analyzes the observed outliers, compares the two prototype iterations and the present method with previous work, and considers the implications for manufacturing tolerances and the limitations of the study. Finally, Chapter 8 revisits the research questions and summarizes the main conclusions.

2

Previous Work

This chapter reviews previous work on robot joint zeroing and calibration, and positions the present thesis relative to it. The existing approaches are grouped into service-oriented zeroing methods, broader kinematic calibration techniques, and recent methods that reduce reliance on external metrology. The review focuses on the trade offs between accuracy, cost, and complexity that motivate the narrower problem addressed in this work.

2.1 Zeroing methods

Previous work on robot joint zeroing has generally approached the problem through either service mastering procedures, dedicated joint-offset calibration systems, or broader kinematic recalibration methods. In industrial practice, manufacturers often solve the problem through reference-based mastering. ABB service documentation describes calibration by moving robot axes to synchronization markings and then updating the revolution counters in the controller. Universal Robots similarly describes joint zeroing after joint replacement either through an automatic calibration procedure or manually by aligning the joints with simple physical references and a spirit level. These approaches are practical and suitable for service, but they rely on built-in reference features and manual alignment, which may limit achievable absolute accuracy. [1] [2] In research, one common approach has been to estimate joint zero offsets using external optical measurement, in which a laser mounted on the robot end-effector interacts with one or more position sensitive devices (PSDs).[Liu and Xi, 2011] propose a low-cost method based on a single-point constraint, reporting a localization error within 2 μm. [Gao et al., 2014] extend this idea with a virtual linear constraint method, using a portable dual-PSD setup to magnify small pose

[1] Information retrieved from ABB website: `https://search.abb.com/library/Download.aspx?DocumentID=3HAC044266-001\&LanguageCode=en\&DocumentPartId=\&Action=Launch`

[2] Information retrieved from URobots website: `https://www.universal-robots.com/manuals/EN/HTML/SW5_19/Content/prod-serv-man/E-series/serv-man-joint-zeroing.htm`

changes and identify joint zero offsets from the recorded joint angles. These methods show that joint offset calibration can be made portable and relatively fast, but they still depend on dedicated optical hardware, calibration routines, and identification algorithms.

2.2 Broader Calibration Approaches

To compensate for geometric and systematic errors, industrial robots are commonly calibrated using external measurement systems. Established calibration approaches include laser tracker-based methods, photogrammetry, vision-based systems, and contact probing techniques. [Elatta et al., 2004] These methods aim to identify deviations in kinematic parameters and update the robot model accordingly. While such techniques can significantly improve absolute accuracy, they are typically associated with high cost, specialized equipment, and controlled environments.[Wu et al., 2023] As a result, they are not well suited for frequent recalibration in service environments, motivating research into alternative approaches such as joint-level zeroing.[Kana et al., 2022] The solution for this, proposed in this paper, is prompted by a very practical need, a way to re-zero joints in a cost-effective and efficient way in an industrial environment.

Another major line of previous work treats zero offsets as part of a complete kinematic calibration problem. In these methods, the objective is not only to identify encoder offsets, but also to estimate additional geometric parameters such as link dimensions, axis orientations, and other error terms. [Kana et al., 2022] describe this as the dominant framing in the literature and note that many methods rely on external measurement devices or mechanical fixtures. This class of methods can improve absolute accuracy substantially, but it is usually more complex than a pure service-zeroing procedure and is therefore less attractive for fast recovery after maintenance.

More recent research has also investigated calibration methods that reduce reliance on external metrology systems. [Petrič and Žlajpah, 2023] presented a kinematic calibration approach for a collaborative redundant robot based on a closed kinematic chain with a spherical joint. In contrast to conventional calibration methods using laser trackers or specialized external fixtures, their method uses internal mechanical constraints and robot motion to obtain calibration data. This makes the approach more cost-effective and easier to deploy in practical environments. Nevertheless, the work remains focused on full kinematic calibration of the robot model, rather than on the narrower maintenance problem of re-establishing an accurate joint zero position after replacement of an individual joint.

2.3 Summary

Taken together, previous work shows that joint zero errors are usually addressed in one of four ways, by mastering against mechanical reference marks, by using external optical systems to estimate joint offsets, by performing full kinematic recalibration, or by using closed kinematic chains to collect calibration data. However, fewer methods are aimed specifically at a robust, low-complexity, service oriented zeroing solution for modular joint replacement in industrial environments. This thesis therefore focuses on a narrower problem than full calibration. Establishing joint zero offset with sufficiently high repeatability and precision so that the need for complete robot recalibration can be removed after maintenance.

3

Theoretical Background

This chapter introduces the theoretical concepts underlying the rest of the thesis. It covers the kinematics of serial manipulators, how forward kinematics maps joint variables to the tool center point, and how joint zero offsets propagate through the kinematic chain to produce positioning errors. The chapter also defines the distinction between accuracy and repeatability and outlines the mechanical and measurement considerations relevant to a high-precision zeroing system.

3.1 Robot Kinematics and Error Propagation

Industrial robotic manipulators are typically modeled as serial kinematic chains consisting of rigid links connected by actuated revolute joints. The pose of the tool center point (TCP) is determined through forward kinematics, which maps joint variables and geometric parameters to a Cartesian position and orientation [Craig, 2005]. In an idealized model, the TCP pose is uniquely defined by the joint angles and nominal link parameters. In practice, however, deviations from this model introduce positioning errors. These deviations originate from multiple sources, including geometric parameter inaccuracies, joint compliance, thermal effects, and encoder-related offsets[Elatta et al., 2004]. Among these, joint zero offsets represent a particularly critical error source. An angular offset at any joint propagates through the kinematic chain and results in a displacement at the TCP. For sufficiently small angular deviations, this relationship can be approximated linearly, where the resulting TCP error is proportional to the product of the angular error and the effective distance from the joint to the TCP[Mooring et al., 1991]. Consequently, errors in proximal joints, which possess longer effective lever arms, produce significantly larger TCP deviations than equivalent errors in distal joints. This non-uniform error amplification is a fundamental characteristic of serial manipulators.

3.2 Forward Kinematics

Forward kinematics describes how the pose of a robot's end-effector is computed from its joint variables. Let the vector of joint variables be

$$q = [q_1, q_2, ..., q_n]^T,$$

where q_i is a joint angle for a revolute joint or linear displacement for a prismatic joint. The forward kinematics problem is to determine the end-effector pose

$$X = f(q),$$

where X represents a suitable representation of both position and orientation. The mapping is deterministic and is obtained by combining the geometric effect of each joint and link in sequence, expressed as a product of homogeneous transformation matrices

$$^0T_i = ^0T_1 ^1T_2 ... ^{i-1}T_i$$

where frame 0 is chosen as the robot base fram and serves as reference for all transformations. A standard convention for defining each transformation $^{i-1}T_i$ is the Denavit-Hartenberg (DH) convention, which parametrizes the relative motion between consecutive frames using four quantities per link, the link length r_i, the link twist α_i, the link offset d_i, and the joint angle θ_i[Craig, 2005]. For a revolute joint θ_i is the variable, for a prismatic joint d_i is the variable. Forward kinematics provides the foundation for analyzing how deviations in joint variables, such as zero offsets, propagate through the kinematic chain to the TCP. The standard tool for this analysis is the manipulator Jacobian, which linearizes the forward kinematic mapping around a given configuration q. The geometric Jacobian $J(q) \in \mathbb{R}^{6\times n}$ maps joint velocities directly to end-effector linear and angular velocities, both expressed in the base frame, and is independent of the chosen orientation parametrization [Mooring et al., 1991]. Since the accuracy requirement in this thesis is defined in terms of TCP position, only the linear part $J_v(q) \in \mathbb{R}^{3\times n}$ of the geometric Jacobian is needed. Denoting the TCP position by $p \in \mathbb{R}^3$, the position displacement resulting from a small joint deviation δq is approximated as

$$\delta p \approx J_v(q) \cdot \delta q \tag{3.1}$$

This first order relationship forms the basis for the joint-zero-offset sensitivity analysis in Chapter 4.

3.3 Joint Zero Offset and Absolute Positioning Accuracy

The joint zero offset is defined as the deviation between the encoder-defined electrical zero and the true mechanical reference position of a joint. During operation,

the encoder provides relative angular measurements, and the absolute reference is established during a zeroing procedure[Mooring et al., 1991]. Any inaccuracy introduced at this stage becomes an error embedded in the robot's kinematic model. Unlike random disturbances, joint zero offsets are deterministic and persist across all motions, directly degrading the absolute positioning accuracy of the robot. [Elatta et al., 2004]

3.4 Absolute Accuracy and Repeatability

Two fundamental performance metrics in industrial robotics are absolute accuracy and repeatability. Absolute accuracy refers to the deviation between the commanded and the actual TCP position in a coordinate frame, while repeatability describes the robot's ability to return to the same position under identical conditions. Industrial robots typically exhibit high repeatability but comparatively lower absolute accuracy. This is because repeatability depends primarily on internal consistency, whereas absolute accuracy depends on the correctness of the kinematic model, outside effects, and its calibration. Joint zero offsets directly affect absolute accuracy but have minimal influence on repeatability, as the offset remains constant across repeated motions.[Mooring et al., 1991]

3.5 Mechanical Precision and Structural Considerations

Achieving micrometer-level positioning accuracy requires careful consideration of mechanical design principles. Key factors include tolerance stack-up, elastic deformation, thermal expansion, and contact mechanics. Tolerance stack-up refers to the accumulation of dimensional variations across components, which can significantly affect system accuracy. Elastic deformation under load introduces compliance, while thermal expansion alters geometry under temperature variation. Contact mechanics govern how surfaces interact and settle into a repeatable position. Designs that employ deterministic constraints and well-defined contact interfaces can achieve high repeatability.

3.6 Measurement Resolution

The achievable accuracy of a joint zeroing system is constrained by both the sensor resolution and mechanical repeatability. Encoder resolution defines the smallest measurable angular increment. However, in many practical systems, the dominant limitation arises from mechanical uncertainty rather than sensor resolution[Mooring et al., 1991]. As a result, improving mechanical alignment and fixture stability is often more critical than increasing sensing precision.

4

System design

This chapter describes the development of the joint zeroing system, from the definition of quantitative accuracy requirements through concept selection to the final machined design. The objective was a substantial increase in zeroing accuracy, sufficient to reduce or eliminate the need for full robot recalibration after joint replacement, rather than an incremental improvement of the existing procedure. Development began with a review of the current zeroing process, establishing how the mechanical reference features are aligned and how the zero position is stored in firmware.

4.1 Requirements Analysis

Joint Overview

The zeroing of the joints in question is based on reference pin alignment. A simplified depiction of the joint is displayed in Figure 4.1a, 4.1b, and 4.1c. The joint is in zero position when a line between the pins on top is parallel to a line between the pins on the bottom or rotated 3.5° from the parallel position depending on whether the joint will be mounted in the base- or shoulder of a robot Figure 4.1d.

Accuracy Requirement

The first step was to determine the required zeroing precision of the joint reference pin. A sensitivity analysis was performed for all robot configurations to estimate the relationship between joint zero error and resulting TCP error. Considering realistic manufacturing tolerances and feasibility, targets of $6 - 30\mu m$ at the pin were evaluated. In principle, the relationship between joint zero offsets and the resulting TCP error can be derived rigorously using the forward kinematic model of the robot. Each joint zero offset δq_i enters as a deviation to the joint angle θ_i in the corresponding DH transformation matrix ${}^{i-1}T_i$, and the resulting TCP displacement can be obtained either by recomputing the full forward kinematics with deviated angles or, similarly, through the manipulator Jacobian $\delta p \approx J(q)\delta q$. This approach captures the full three-dimensional geometry of the robot, including the contribution of

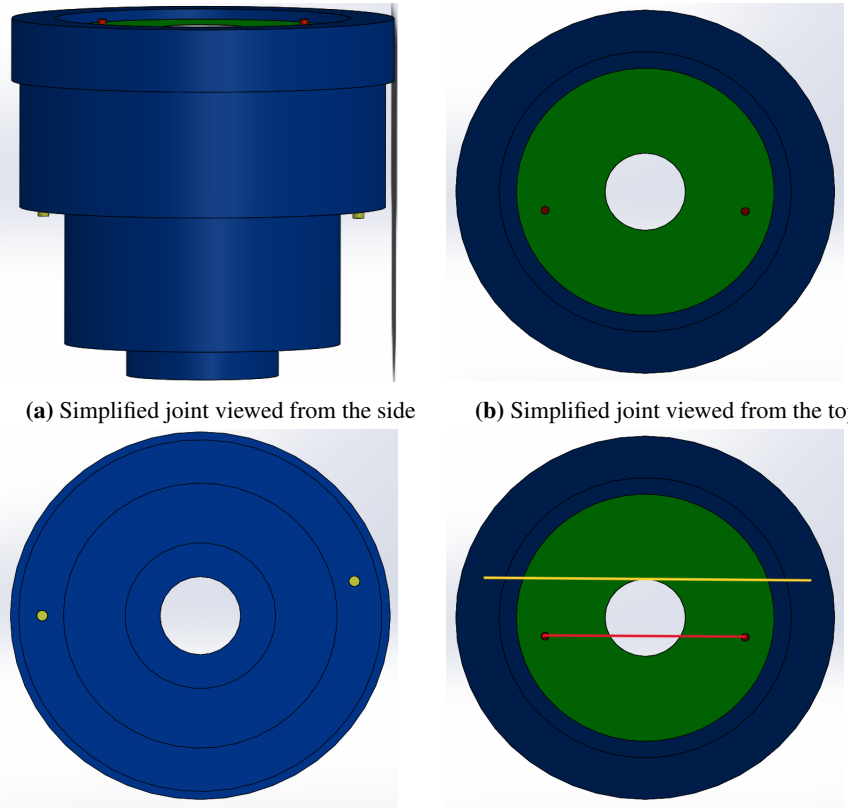

(a) Simplified joint viewed from the side

(b) Simplified joint viewed from the top

(c) Simplified joint viewed from the bottom

(d) Simplified joint with lines between pins.

Figure 4.1 The green part is the output of the joint, the red parts are the pins connected to the output, the yellow parts are the pins connected to the housing, and the blue part is the housing.

every joint along the kinematic chain. For the purpose of deriving the zeroing accuracy required at a single joint, however, the full Jacobian formulation introduces complexity that is not justified. Each joint can instead be analyzed in isolation as a rotational pivot with an effective lever arm to the TCP, where a small angular deviation $\delta\theta$ produces an arc displacement that, for small angles, is approximately linear in the lever arm length. This reduces the analysis to a single-joint sensitivity expression that is straightforward to evaluate across all joints and robot configurations. A Python script was developed to evaluate the TCP error resulting from a given pin displacement for each joint across all robot configurations. The underlying geometric relationship is illustrated in Figure 4.2. For a small angular deviation $\delta\theta$ at the joint, the pin located at radius r from the joint center is displaced by $d = r \cdot \delta\theta$. The corresponding TCP displacement, for an effective lever arm of length L from the

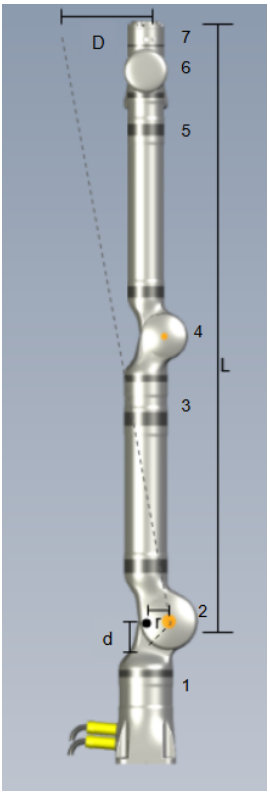

Figure 4.2 Geometry of the system showing length L, TCP travel distance D, pin travel distance d, and radius from joint center to pin r. The numbers in the figure corresponds to the joints numbers and position in the robot.

joint to the TCP, is

$$\frac{D}{L} = \delta\theta = \frac{d}{r} \Rightarrow D = \delta\theta \cdot L \tag{4.1}$$

where D is the TCP distance[mm], L is the distance from the joint to the TCP[mm], d is the pin displacement[mm] and r is the radius from joint center to the pin[mm]. The calculated TCP errors for each joint and robot configuration, assuming a pin accuracy of 20μm, are shown in Figure 4.3. The equation above was evaluated for multiple candidate pin accuracies to determine the minimum requirement. Engineering practice at Kassow Robots indicates that a joint zeroing accuracy sufficient to achieve a TCP positioning error below 1 mm is adequate, as residual assembly variations, such as play in the base mounting screws, typically introduce deviations of comparable magnitude regardless of joint zeroing precision. A station-specific calibration is therefore still required for each deployment, but a full dynamic robot recalibration can be avoided. The results show that a pin accuracy of 20μm yields a

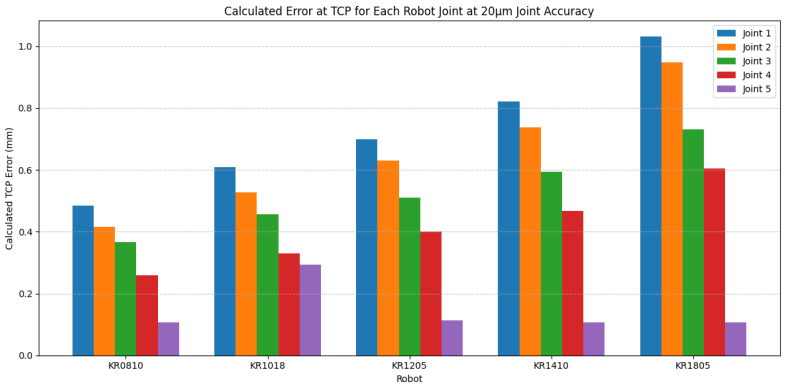

Figure 4.3 Calculated error at TCP with 20μm accuracy at pin. Calculation performed for each joint in 5 different sizes of robots, from smallest to largest.

TCP error below 1 mm for all robot configurations, with the exception of the base joint in the largest robot. The base joint requires the most accurate pin position due to its longest effective lever arm. The base joint of the largest robot was therefore selected as the prototyping target, since a design validated for this configuration can be scaled to the remaining joints.

Encoder Resolution

The achievable measurement resolution of the system is bounded by the encoder resolution. The joint encoder provides an angular resolution of $2^{-31} \cdot 2147$ rad, or approximately 1μrad. At the reference pin with radius r = 38 mm, this corresponds to a linear resolution of approximately $\tan(1 \cdot 10^{-6}) \cdot \mathrm{r} = 38 \cdot 10^{-9}$, or 38 nm, which is more than two orders of magnitude finer than the 20 μm pin-accuracy target. The encoder resolution is therefore not a limiting factor, and the system's repeatability is governed by mechanical rather than sensing precision.

4.2 Concept Generation and Selection

Based on the derived accuracy requirements, three candidate concepts were identified: a fully mechanical fixture, a triangulation-laser based measurement system, and a vision-based solution. A qualitative comparison of the three concepts is presented in Table 4.1

Mechanical solution

Several mechanical concepts were explored before settling on a final candidate. The initial idea was a clamping arrangement that would close around the joint and locate the reference pin against a precision-machined stop. This was rejected early due to

Criteria	Mechanical	Laser	Camera
Hardware cost	Low	High	Medium
Software complexity	Low	High	High
Sensitivity to environment	Low	High	High
Machining accuracy required	High	High	Medium
Industrial Robustness	High	Medium	Medium
Achievable precision	High	High	Medium

Table 4.1 Table with initial pros and cons of the three concepts

concerns about reliability and the contact forces required to hold the joint securely without inducing deflection in the fixture. A side-mounted alignment fixture was considered next, in which a precision-machined feature would approach the joint from the side and locate the pin laterally. This avoided the clamping forces of the first design but introduced a single-sided contact that was sensitive to the direction of the applied torque, raising concerns about repeatability of the contact geometry. A third concept was a geometric stop resembling a ratchet, with protruding walls arranged in a circle around the joint at the correct angular position. This approach was attractive because it provided a passive, contact-defined zero position without active clamping. However, the small contact area between the pin and the stopping wall raised concerns about the local deformation and tolerance of the contact surface, both of which would limit achievable repeatability. Kinematic coupling principles were also considered as a means of achieving micron level repeatability through deterministic constraint of all six degrees of freedom. While theoretically attractive, a strict kinematic coupling would either require the joint itself to be designed around the coupling, which was outside the scope of this thesis, or accept very small contact patches with high local stresses, leading to deflection under the torque applied during zeroing. The selected concept addresses these issues. The joint is located in a cup-shaped base fixture that provides high rotational stiffness through a large, distributed contact surface. The zero position is defined by a loosely mounted block on top, which has controlled degrees of freedom and is driven into its locked position by the joint's own rotational motion during the zeroing procedure. The detailed development of this concept is described in Section 4.3.

Laser solution

Laser triangulation sensors were investigated as a potential high-resolution measurement solution. Industrial sensors with micron level resolution were identified from at least two European suppliers, with quoted prices around 1243 EUR per unit. Three main measurement strategies were evaluated. The first strategy measured the lateral displacement of a protruding pin using laser placed perpendicular to the pins direction of movement. The second strategy measured along the direction of motion and identified the apex of the rounded pin by analyzing the rate of change in distance. The third strategy used two calibrated perpendicular lasers to derive the

position of the pin. In all three cases, the measurement could in principle be improved by sampling multiple points across the pin surface and fitting a parabola to identify the geometric minimum, raising the effective resolution beyond the single-point sensor specification. Resolution on the order of 1μm seemed feasible in principle. However, several limitations were identified. The sensor cost exceeded 1200 EUR per unit, reflective surfaces require a 19° incidence angle which was difficult to maintain on a curved pin surface, the beam divergence would cover more than half the radius of the pin and therefore loses precision, and additional mechanical fixtures of high accuracy were still required to position the sensors. The approach also required substantial software development for measurement filtering, surface modeling, and parabola fitting to ensure measurement robustness. The combined cost and complexity were not competitive with the mechanical concept.

Camera solution

A vision-based approach was also briefly evaluated. The concept involved detecting the angular position of the reference pin through image processing, with two candidate strategies. The first relied on a precisely fixed camera orientation, where the pin's angle could be measured directly relative to the image frame. This required the camera to be rigidly mounted and rotationally calibrated, and any drift in mounting orientation would translate directly into measurement error. The second strategy used a secondary reference feature in the image, a separate fixture marker or geometric reference, against which the pin position could be measured relatively, removing the dependence on absolute camera orientation but introduce the need for a second precision feature in the field of view. Both strategies were technically plausible but raised concerns about calibration repeatability, sensitivity to ambient lighting and surface reflections, and achievable accuracy in an industrial environment. Without a clear advantage over either the mechanical or laser concepts on cost, robustness, or precision, the camera approach was not developed further.

Concept Selection

Following comparative evaluation of accuracy potential, cost, robustness, and industrial feasibility, the mechanical approach was selected as the primary development direction. The decision was motivated by lower system complexity, independence from sensitive optical components, potential for high repeatability through well-defined contact geometry, and better alignment with industrial production constraints.

Working Principle. The selected concept is based on a passive self-locking mechanism that drives the joint into a single, repeatable angular position using the joint's own motion. The principle is illustrated in Figure 4.4a, with the contact forces shown in Figure 4.4b. In the figures, the filled circles represent the pins on the output of the joint, the dotted circles represent the pins on the housing at the bottom of the joint, and the hatched surfaces represent the contact reference features of the

fixture. The mechanism relies on three sets of contact features. The output of the joint carries pins on its top face, the housing carries pins on its bottom face, and the cup-shaped base fixture carries fixed reference pins on top and flat contact surfaces in the bottom of the cup-shape. A loosely mounted block is placed on top of the joint, positioned between the output pins and the fixed reference pins of the fixture. The block is not clamped or located precisely by hand; it is free to move within controlled limits and is brought into position by the rotational motion itself. When a low torque is applied, the joint output rotates and the output pins drive against flat faces on both sides of the loose block. The block is pushed until it contacts the fixed reference pins of the fixture, at which point it can no longer rotate. Because the block is now constrained between the moving output pins on one side and the fixed reference pins on the other, the continued application of torque transfers the reaction through the block and into the housing, rotating the housing until its bottom pins seat against the cut-outs in the base of the cup. At this point every element in the chain is constrained against the fixed fixture, and the joint can rotate no further. The angular position reached is 69.86° offset from the true zero position, and the encoder reading is recorded there. The angular offset of 69.86° is added in software for the correct zero position to be saved in the joint's firmware. The repeatability of the mechanism comes from how the block is constrained when it settles. The contact surfaces between the block, the output pins, and the fixed reference pins are arranged so that they are mutually parallel or perpendicular. As a result, the block is constrained in every direction in the plane, and there is only one geometric position in which all contacts are satisfied simultaneously. The block therefore self-centers into the same position on every cycle, independent of how it was initially placed. Figure 4.4b shows the corresponding force balances. When the block is correctly seated, the contact forces acting on it are equal and opposing, so there is no residual force driving further motion and the block is held statically in place. Friction is neglected in this analysis, as the contact forces are dominated by the applied torque and the friction contribution is small in comparison. The cup-shaped base provides high rotational stiffness through the circular geometry. This geometry also reduces the impact of thermal effects on the zeroing, since the material expands or contracts equally in all directions in the plane. The zero position itself is defined entirely by the deterministic contact between the block and the reference pins. This separation means that high zeroing repeatability does not depend on the cup being manufactured to extreme tolerances, only on the contact geometry of the block and pins, which is a far smaller and more controllable set of features.

A refined mechanical concept was developed in which the joint is placed in a cup-shaped fixture providing high rotational stiffness, while a loosely mounted block utilizes controlled degrees of freedom and rotational forces to self-lock into the correct position during the joint's rotational movement.

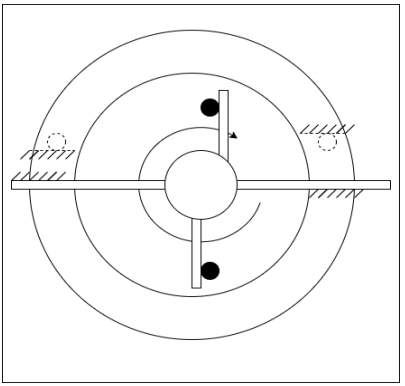

(a) Initial mechanical concept.

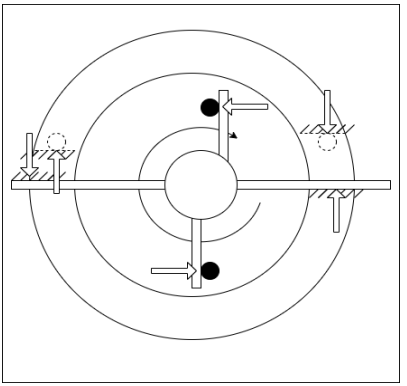

(b) Initial mechanical concept with forces canceling out when the stopper on top is in the right position.

Figure 4.4 The filled in circles represent the pins on the output, dotted circles represent the pins on the bottom of the joint. The rotational arrow describes the rotational motion of the output, which moves the pins on the output. The middle circle and the rectangular beams represent the loose block on top.

4.3 Detailed Design and Prototyping

CAD models were developed to refine the geometry of the fixture and stopping mechanism. Structural considerations included contact surface geometry, stiffness of supporting structure, and material selection. A material comparison was carried out to select suitable materials for the fixture components. Input parameters included the torque output of the joint, expected thermal variation, and the cross-sectional dimensions of the design, all derived from early design concepts and joint specifications. Although the cross-sectional dimensions were subsequently refined and the fixture geometry became circular, making thermal expansion less problematic, the resulting material ranking remained valid.

Prototype Development

A first prototype of the mechanical fixture was produced by 3D-printing to enable rapid iteration. During early testing, several design refinements were identified, increased contact-surface area to reduce rotational play, cable routing cut-outs to prevent interference with joint wiring, and geometric simplification to improve manufacturability and dimensional accuracy. A second prototype iteration incorporated a sliding base compatible with the zeroing station and refined alignment features, replacing rounded cut-outs with locating pins, see Figure 4.7.

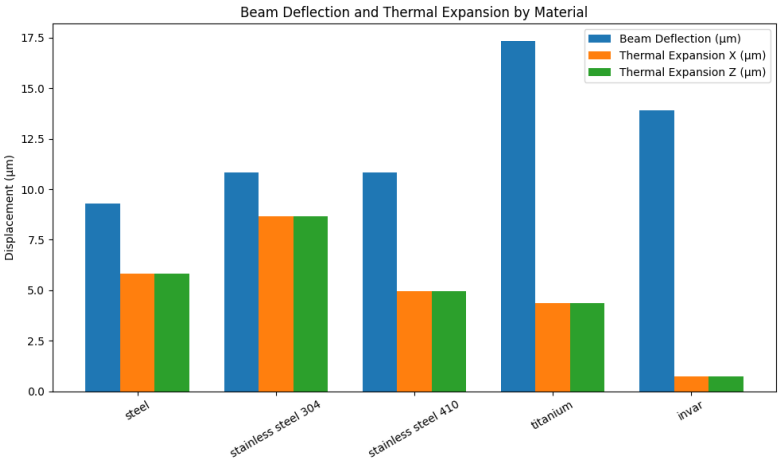

Figure 4.5 Calculated Material Deformation of Different Materials

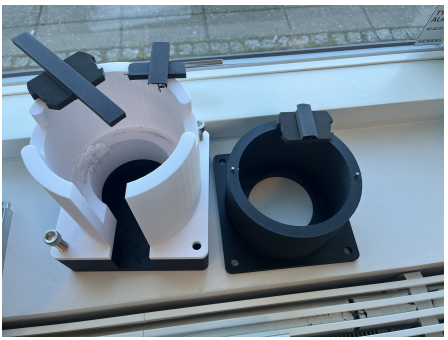

Figure 4.6 First prototype in white (left) and second refined prototype in black (right)

Final Design

The final design consists of two main components: a cup-shaped base fixture and a loose block on top. The self-locking block, see Figure 4.8, mounted with controlled degrees of freedom, engages the reference pin during the joint's rotational motion and self-locates into the reference position under the applied torque. The cup-shaped fixture, see Figure 4.9, provides high rotational stiffness and locates the joint housing through a precision-machined contact surface. Figure 4.10 shows the assembled fixture with the joint mounted ready to be zeroed.

The final fixture geometry was machined from stainless steel 410, with critical contact surfaces ground to a tolerance of 5μm to ensure repeatable contact. A cable routing cut-out was incorporated to prevent interference with joint wiring during insertion and to prevent sensitive wires from getting clamped and trapped between

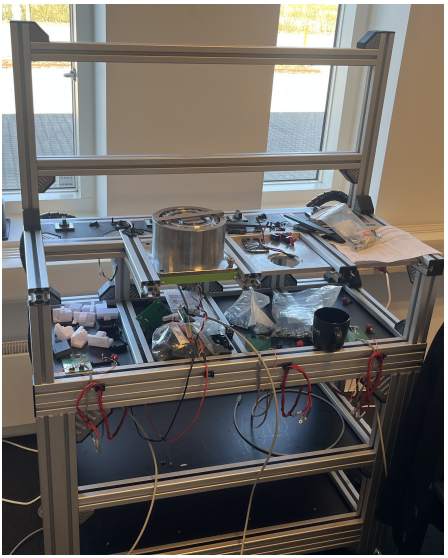

Figure 4.7 Experimental zeroing station used for quantitative testing of the zeroing fixture.

Figure 4.8 Picture of the self-locking block that will be placed on top.

the joint and the fixture.

Material selection was finalized based on the results from the calculations in Figure 4.5, balancing deflection under load, thermal stability, and manufacturability. Stainless steel 410 was selected due to its favorable trade-off between low thermal expansion, stiffness, manufacturability, price, and availability.

Control Integration and Software Support

In parallel with mechanical development, software tools were implemented to enable controlled joint motion and data acquisition. A script was developed to interface with Kassow's joint calibration and zeroing GUI to control the joint under test.

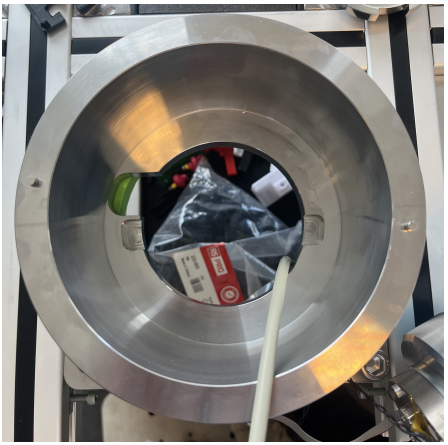

Figure 4.9 Picture of the final cup-shaped mechanical fixture. The pins on the bottom of the joint gets placed into two shallow cut-outs and the through hole is designed for cables.

Key challenges included extracting and logging encoder data in CSV format and ensuring consistent motion control for repeatable testing.

4.4 Future Improvements

Several improvements have been identified for future iterations of the design, based on observations made during prototype testing. Three major improvements will be explained below.

First, the current design is dimensioned for the base joint of the largest robot configuration. A scaled family of fixtures covering all joint sizes in the Kassow product range would be required for full production deployment. The geometric scaling is straightforward, but each fixture would require independent verification.

Second, the current design has limited usability in a production setting. Joint insertion and removal require careful handling of the joint wiring and precise alignment with the fixture, which is challenging given the weight of the joint. Inverting the assembly, such that the joint is mounted upright and the cup fixture is lowered onto it from above, would simplify handling, reduce strain on the wiring, and improve operator ergonomics without altering the underlying mechanical principle.

Finally, the long-term durability of the contact surfaces has not been studied. The reference pins are loaded against the locking block during every zeroing cycle, and repeated contact under torque is likely to cause gradual wear over the service life of the fixture. Introducing hardened or coated inserts at the contact interfaces could extend the lifetime of the fixture without affecting the underlying geometry, and would also reduce sensitivity to occasional debris or surface contamination on the contact faces. This is particularly relevant for production environments where

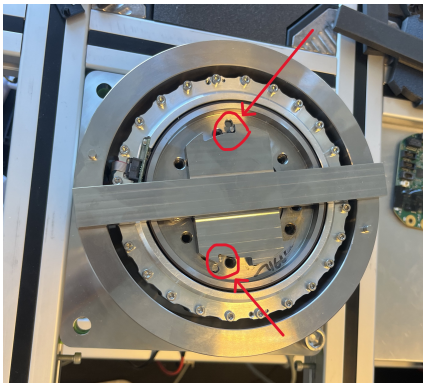

(a) Fixture in zeroing station from top view and output pins pointed to for clarity.

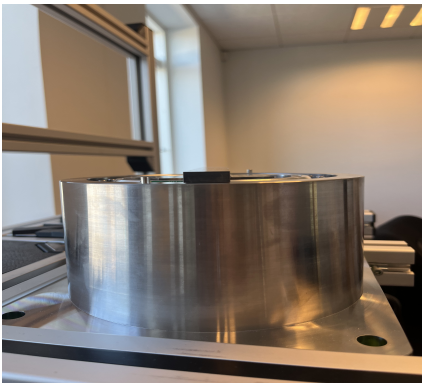

(b) Fixture in zeroing station from side view

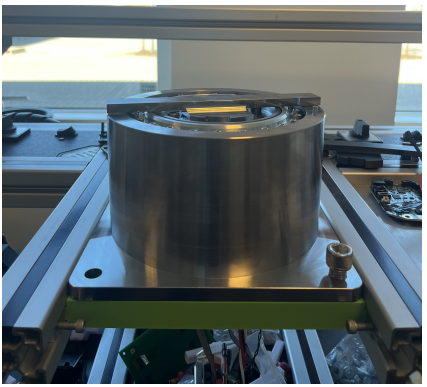

(c) Fixture in zeroing station from front view

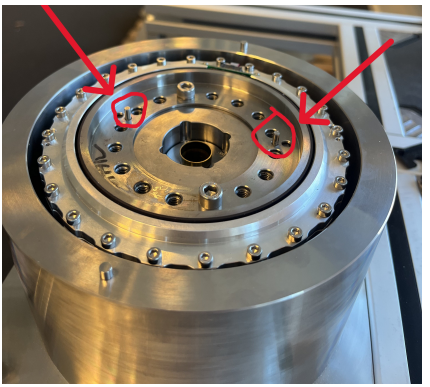

(d) Fixture in zeroing station without top and output pins pointed to for clarity.

Figure 4.10 Three views of the cup-shaped fixture with the joint seated inside and the loose self-locking top on top and last picture without the top.

the fixture is expected to perform large numbers of zeroing cycles between maintenance intervals.

5

Testing

The purpose of the testing phase is to evaluate whether the developed joint zeroing system meets the required precision, repeatability, and robustness for the industrial application.

5.1 Experimental Setup

Testing was carried out in two stages, using two physical iterations of the fixture: an initial 3D-printed prototype and a subsequent CNC-machined metal version. Both iterations were tested using the same procedure on the experimental zeroing station shown in Figure 4.7. The fixture was rigidly mounted to the station base, with the robot joint seated in the cup-shaped base and the self-locking top placed loosely on the output. The joint was actuated through its dedicated controller, and a custom software interface was developed to issue motion and torque commands and to log encoder data in CSV format. The encoder resolution of approximately 1μrad ensured that mechanical repeatability, rather than measurement resolution, was the limiting factor. The geometrical limitations from the design, caused the self-locking block to be stopped at 69.86° from the zero position, this offset was added in software as described in Step 7.

5.2 Test Procedure

A single zeroing cycle followed the procedure below. The cycle was implemented in software to ensure that all steps were executed identically across trials.

1. Seat the joint in the cup-shaped base fixture
2. Rotate the joint output into a position that allows the self-locking top to be placed on the joint without contacting the reference pins.
3. Place the self-locking top on the joint output.

4. Issue a low-torque command to the joint, set to the minimum torque that reliably initiates output rotation. This drives the locking top into contact with the reference pins.

5. Detect zero output velocity for one continuous second, indicating that the locking top has settled against the pins. Record the encoder position at this point.

6. Issue a position command to rotate the output back by 0.2 rad to disengage the self-locking top, allowing it to be removed without disturbing the joint.

7. Apply the joint-specific zero offset to the recorded encoder position. The offset is 69.86° for the base joint and $69.86^\circ + 3.5^\circ$ for the shoulder joint, accounting for the geometric differences described in Section 4.1.

8. Repeat steps 4-7 three times. The first iteration of each test sequence is discarded to compensate for a known firmware behavior that introduces a one-time offset on the first run after fixture engagement.

5.3 Repeatability Test

Repeatability was evaluated by performing 35 and 96 consecutive zeroing cycles on the same joint with the 3D-printed fixture and the metal fixture respectively. This was done without removing the joint from the fixture between cycles. The recorded encoder values were compared, and the spread was characterized by the standard deviation and peak-to-peak variation. This test isolates the repeatability of the mechanical locking action itself, independent of joint insertion variability. The recorded encoder values are converted to pin-level displacement using the known pin radius and propagated to TCP error via Equation (4.1), enabling direct comparison with the 1 mm TCP requirement.

5.4 Reproducibility Test

A second test was performed to assess the contribution of joint insertion to the overall zeroing uncertainty. In contrast to the repeatability test, the joint was removed from the fixture and reinserted after every third zeroing cycle, so that the recorded data captures both the repeatability of the locking mechanism and the variability introduced by re-seating the joint. The software function responsible for the setup offset identified in the repeatability test had been removed prior to this test, allowing its negative effect to be verified.

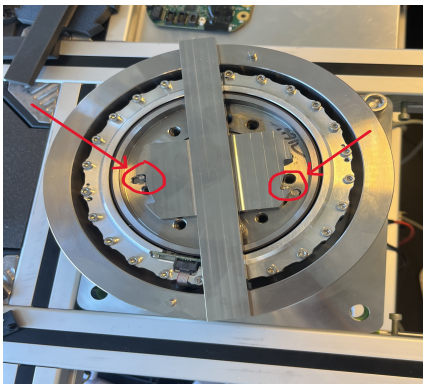

(a) Fixture in zeroing station from top view and output pins pointed to for clarity.

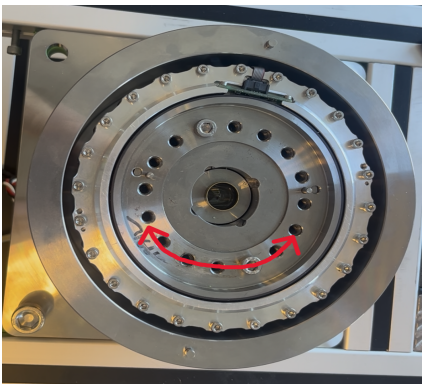

(b) Step 2: Rotate the joint into a position that allows top to be placed.

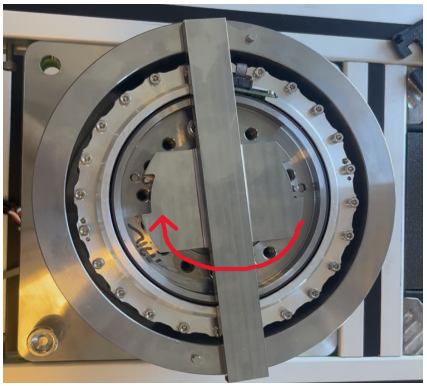

(c) Step 3: Place the top into position

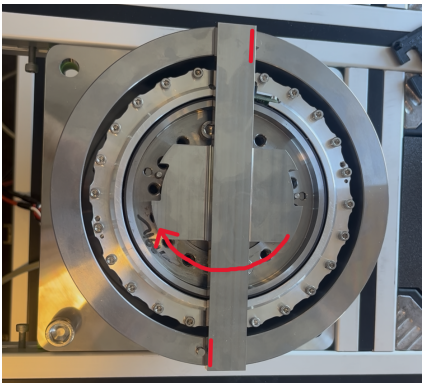

(d) Step 4: Output rotating with low torque until contact with pins (In the figure, contact has only been realized with outer pins on top)

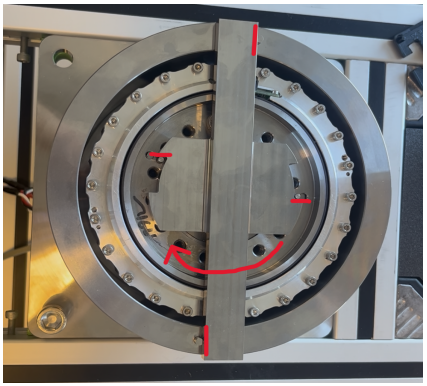

(e) Step 5: Joint in locked position, encoder readings saved.

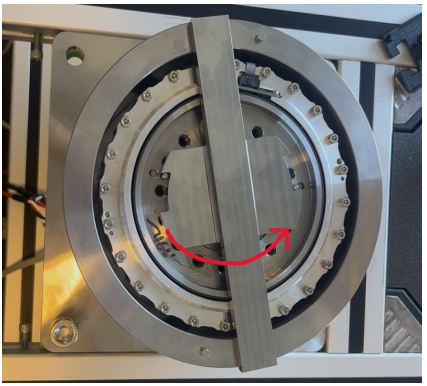

(f) Step 6: Output rotated counterclockwise to release tension and make top removable.

Figure 5.1 Figures showing the step-by-step of the testing method.

6

Results

This chapter presents the results of the repeatability tests described in Chapter 5, performed on both the 3D-printed prototype and the CNC-machined metal fixture. The results are evaluated against the TCP positioning error requirement of below 1 mm derived in Section 4.1. A short cost analysis of the machined prototype is included at the end of the chapter.

Repeatability of the 3D-printed Prototype

Across 35 consecutive zeroing cycles with the 3D-printed fixture, the recorded encoder positions exhibited a standard deviation of 0.124° at the joint output, corresponding to approximately $\pm 82\mu$m of variation at the reference pin and a TCP-level spread with standard deviation of approximately 4.55mm. Encoder positions ranged from -0.314° to 0.317° from the predicted zero position, a peak-to-peak span of 0.63° corresponding to a TCP error range exceeding 23mm.

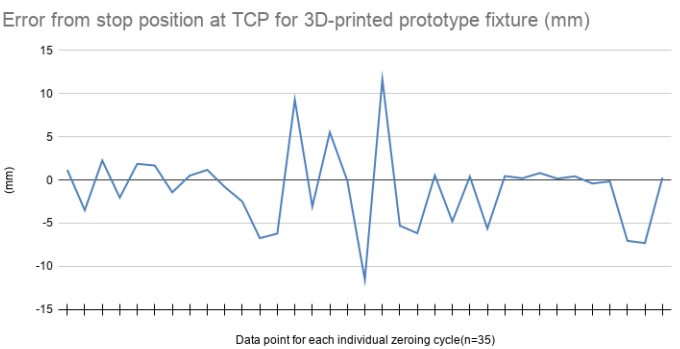

Figure 6.1 Distribution of recorded encoder positions for the 3D-printed fixture, translated to mm at TCP

Summary of Repeatability Results

A summary of the results from both fixtures is presented in Table 6.1 and a comparison plot of 3D-printed and metal fixture in Figure 6.2.

Quantity	**3D-printed (n=35)**	**Machined, all (n=96)**	**Machined, cleaned (n=89)**	**Requirement**
Std. dev. (encoder)	0.124°	0.054°	0.010°	–
Std. dev. (pin)	82μm	36μm	3μm	$< 20\mu$m
Std. dev. (TCP)	4.55mm	0.38mm	0.18mm	$<$ 1mm
Range (TCP)	23.2mm	3.05mm	1.36mm	$<$ 2mm
Samples within $\pm$1mm (TCP)	13/35(37%)	89/96(93%)	89/89(100%)	–

Table 6.1 Summary of repeatability results

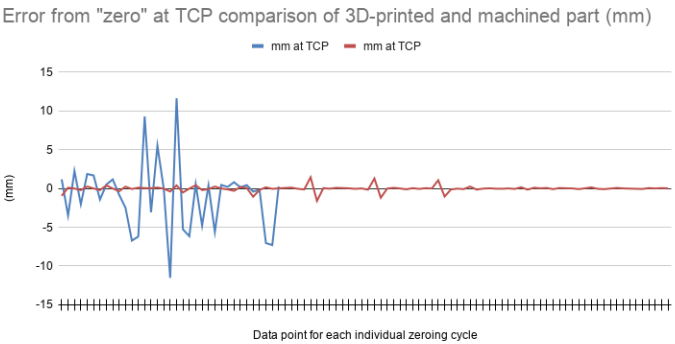

Figure 6.2 Data from 3D-printed fixture (blue, n=35) and machined fixture (red, n=96) in same plot

Repeatability of the Machined Metal Fixture

The machined fixture was tested across 96 consecutive zeroing cycles. The full dataset exhibited a standard deviation of 0.054° at the joint output, corresponding to a pin-level repeatability of approximately 6.9μm and a TCP-error spread with a standard deviation of 0.38 mm. The recorded TCP errors ranged from -1.61mm to $+1.43$mm. Of the 96 samples, seven exhibited an absolute TCP error exceeding 1 mm. The cause of these outliers, and the justification for treating them separately from the remaining cycles, is addressed in Section 7.2. With these seven samples excluded, the remaining 89 cycles show a TCP-level standard deviation of 0.18 mm and a range from -0.96 mm to $+0.40$ mm. During testing some cyclical outliers were identified. The outliers were found to occur each time the system was re-booted. The cause was tracked down to a function in the setup of the software system. During the next phase of testing, reproducibility testing, this function was removed.

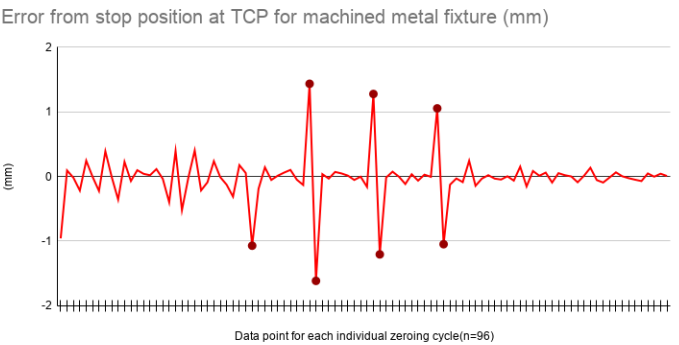

Figure 6.3 Distribution of recorded TCP errors for the machined fixture, translated to mm at TCP, with outliers from software bug indicated.

Reproducibility Under Repeated Joint Insertion

Across 28 cycles, shown in Figure 6.4, with the joint reinserted every third cycle, the machined fixture exhibited an encoder-level standard deviation of 0.0039°, corresponding to a pin-level repeatability of approximately 2.5μm and a TCP-level standard deviation of approximately 0.15 mm. All 28 samples fell within the 1 mm TCP requirement, and no outliers were observed. With the problematic function in the setup removed, the opposite-sign outlier pairs seen in the repeatability test did not reappear.

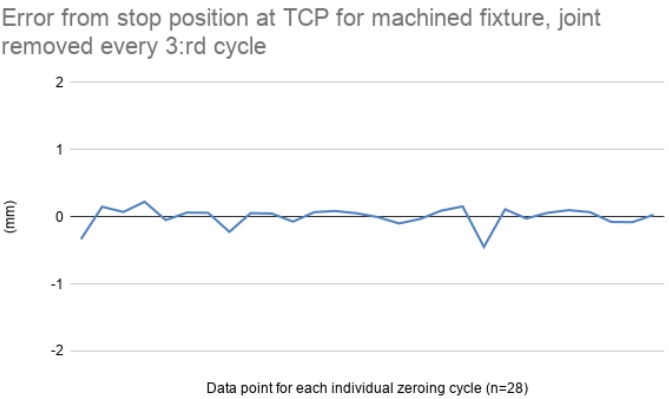

Figure 6.4 Distribution of recorded TCP errors for the machined fixture during reproducibility test, translated to mm at TCP, with the joint re-inserted every third cycles.

Manufacturing Cost

The total manufacturing cost of the machined prototype was 1880 USD, including material, machining, and surface grinding of the contact features. The fixture was produced from stainless steel 316 in a single-piece configuration, with critical contact surfaces ground to a tolerance of 5μm. The cost figure represents a one-off prototype produced in single quantity at a Chinese machine shop.

7

Discussion

This chapter interprets the results presented in Chapter 6. It evaluates the measured performance against the TCP requirement, analyzes the outliers observed in the repeatability test, compares the two prototype iterations, and relates the achieved performance to previous work.

7.1 Performance Against the TCP Requirement

The TCP positioning error requirement of below 1 mm, derived in Section 4.1, is met with substantial margin with the machined fixture. The cleaned dataset of 89 samples shows a TCP-level standard deviation of 0.18 mm, roughly a factor of five below the requirement, and no individual sample exceeds the 1 mm threshold. At the pin level the corresponding standard deviation is approximately 3μm, compared with the 20μm pin-accuracy target derived from the same calculation. The mechanical concept therefore performs significantly better than the level required to avoid full robot recalibration after joint replacement.

This level of performance was not anticipated when the design was specified. Several manufacturing tolerances, in particular the 5μm grinding tolerance on the contact surfaces, were chosen conservatively under the assumption that achieving micrometer-level pin repeatability would require tightly controlled contact geometry. The measured performance suggests that the underlying self-locking mechanism is more forgiving of contact-surface variations than originally assumed. The implications of this for tolerance specification and manufacturing cost are discussed in Section 7.5.

7.2 Outlier Analysis

Of the 96 cycles recorded with the machined fixture, seven samples exhibited an absolute TCP error exceeding 1 mm. These samples were not distributed randomly across the test sequence but appeared in a pattern consistent with the initialization setup procedure and not mechanical noise. After investigation, the cause was traced

to a software function executed during firmware setup that introduces a small offset on the first test run. The function is not part of the zeroing procedure itself and is independent of the mechanical performance of the fixture. It can be removed in future implementations of the test interface without affecting the zeroing mechanism. The seven affected samples are therefore considered non-representative of the mechanical performance of the fixture and have been treated as a separate dataset in the cleaned analysis. Two observations support this treatment. First, the seven outlier samples is cyclical and always occur after the setup function was performed. Second, removing them reduces the TCP-level standard deviation from 0.38 mm to 0.18 mm, a reduction by more than a factor of two, which is consistent with eliminating a single dominant noise source rather than aggressively trimming a distribution. A further observation reinforces this interpretation. Each cycle's encoder reading is computed relative to the zero point established by the preceding cycle, so the recorded values are not statistically independent. A single disturbance in one cycle therefore produces two visible deviations in the dataset: the deviation caused by the disturbance itself, and an apparent deviation of opposite sign in the following cycle, when the reference returns to its undisturbed value. The seven outliers in the dataset alternate in sign in a pattern consistent with this mechanism, which suggests that they correspond to a smaller number of underlying disturbance events, on the order of three or four, each manifesting as a pair of consecutive opposite-sign samples. This further supports the conclusion that the disturbance is a discrete software artifact rather than continuous mechanical noise, and that the mechanical fixture itself contributes negligibly to the observed outlier behavior. It is nevertheless worth noting that, even with the outliers retained, 89 of the 96 samples fall within the 1 mm requirement. This indicates that the underlying mechanical performance is robust enough to absorb a non-mechanical disturbance and still meet the requirement most of the time, which strengthens rather than weakens the conclusion that the fixture is suitable for the intended use case.

This interpretation was subsequently confirmed: with the setup function removed, a separate test of 28 cycles produced no outliers, supporting the conclusion that the disturbance was a software bug rather than a property of the mechanical fixture.

7.3 Comparison Between Prototype Iterations

The two fixture iterations differ by roughly two orders of magnitude in repeatability at every measurement level, despite sharing the same geometry and the same self-locking principle. The 3D-printed prototype shows a TCP-level standard deviation of 4.55 mm against 0.18 mm for the cleaned machined dataset, and a pin-level standard deviation of 82μm against approximately 3μm. The factor by which performance improves between the two iterations is broadly consistent across all three measurement levels, indicating that the limiting factor in the printed prototype is

mechanical stiffness and accuracy rather than any property of the mechanical principle itself. This result has two practical consequences. First, it confirms that the self-locking concept itself is sound, since the same geometry executed with higher manufacturing precision and stiffness delivers a corresponding improvement in zeroing precision. Second it indicates that 3D-printed prototypes are useful for validating concept and procedure but cannot serve as a basis for evaluating absolute performance.

7.4 Comparison with Previous Work

The pin level repeatability of approximately 3μm achieved by the machined fixture is comparable in order of magnitude to the localization errors reported for laser-based joint-offset calibration methods discussed in Chapter 2, which report values in the range of approximately 2μm[Gao et al., 2014]. The present approach achieves this level of repeatability without optical hardware, calibration routines, or identification algorithms, relying instead on a passive mechanical constraint and the joint's own encoder. This supports the framing of the thesis as targeting a different point in the design space than the existing literature: not the highest achievable absolute accuracy, but the highest repeatability achievable with a low-complexity, service-oriented method suitable for industrial maintenance.

7.5 Implications for Manufacturing Tolerances and Cost

The measured performance has direct consequences for the cost of the fixture in a production context. The 1880 USD cost reported in Chapter 6 is dominated by the precision machining of the contact surfaces and the cup geometry, both of which were specified conservatively. With the measured pin level repeatability sitting roughly a factor of seven below the 20μm target, the contact-surface grinding tolerance can plausibly be relaxed without compromising the 1 mm TCP requirement. The exact margin available cannot be determined from the present data alone, since the achieved repeatability is the combined result of manufacturing precision, the locking mechanism geometry, and the joint controller's settling behavior, but the available headroom is substantial. A second, and significant, cost-reduction opportunity lies in the manufacturability of the design itself. The current fixture was machined from a single block with internal features requiring multiple machining setups. A redesign that splits the fixture into a small number of simpler components joined after machining could reduce machining time considerably without compromising the contact geometry that determines repeatability. The redesign that was discussed in Section 4.4, flipping the design upside down could also be beneficial to reduce cost.

7.6 Limitations of the Study

Several limitations of the study should be noted when interpreting the results. First, the reproducibility of the system under repeated joint insertion was evaluated in a separate test, in which the joint was removed and reinserted between cycles, see Chapter 6. This test showed a pin-level repeatability comparable to the in-fixture repeatability test, indicating that joint re-insertion does not significantly degrade zeroing performance. However, this test was limited by time and to a single joint configuration and therefore a relatively small number of insertions. Broader validation across configurations and a larger number of insertion cycles would be needed to fully characterize insertion variability in production. Second, only one fixture geometry, dimensioned for the largest joint situated in the base and shoulder of the largest robot configuration, has been prototyped and tested. While the geometric scaling to other joint sizes is straightforward in principle, scaled fixtures would require independent verification before the conclusions of this thesis can be extended across the full product range. However, the base joint was chosen as it required the most repeatability and we can therefore be optimistic about the concept performing as expected for the smaller sizes. Third, the testing was carried out under stable laboratory conditions over a relatively short timescale. Long-term effects such as wear of the contact surfaces, drift due to temperature variation in a production environment, and degradation under repeated operator handling have not been tested. These effects are likely to be more relevant in industrial deployment than in the validation of the concept. Fourth, the derived results at TCP from the testing was never verified in a full robot. Finally, the comparison with previous work in Section 7.4 is necessarily indirect, since the existing literature targets full kinematic calibration or absolute joint-offset estimation rather than the narrower repeatability problem addressed in this thesis. The reported figures should therefore be read as an order-of-magnitude comparison rather than an exact benchmark.

8

Conclusion

The aim of this thesis was to develop a joint zeroing system accurate enough to avoid full robot recalibration after joint replacement, and feasible to use in a production or service environment. The four research questions from Section 1.3 are revisited below.

Required Zeroing Repeatability. The first question asked what zeroing repeatability is required at the reference pin to keep the TCP error below 1 mm. The sensitivity analysis in Section 4.1 showed that approximately 20μm of repeatability at the pin is sufficient to meet this requirement across the product range. The base joint of the largest robot has the longest effective lever arm and is therefore the most demanding case. It was used as the worst-case reference for the design.

Concept Selection. The second question asked which concepts could meet the accuracy requirement, and how they are compared on cost, robustness, and feasibility. Three concepts were evaluated in Section 4.2, a mechanical fixture, a laser triangulation system, and a vision-based solution. In principle, all three could reach the required precision. The optical solution, however, came with substantial cost, software complexity, and environmental sensitivity, and still required a high-precision mechanical fixture of their own. The mechanical concept was chosen for its lower complexity, its independence from optical components, and the high repeatability achievable through well-defined contact geometry.

Integration with Existing Hardware and Software. The third question asked how the selected solution could be integrated with the existing joint firmware and calibration interfaces without requiring full recalibration. Integration was done through a software interface to the existing joint calibration and zeroing GUI, which allowed automated control of the joint and direct logging of encoder data. No changes to the firmware or to the kinematic calibration procedure were needed. The fixture itself is a passive device that locates the joint mechanically, and the joint's own encoder provides the reference reading. The solution can therefore be added to the existing maintenance workflow, or even the calibration procedure, as a fixture rather than as a new calibration system.

Demonstration of Repeatability and Robustness. The fourth question sought to answer whether the prototype demonstrates sufficient repeatability and robustness to justify industrial implementation. Across 89 representative samples, the machined fixture achieved a TCP standard deviation of 0.18 mm and a pin-level standard deviation of about 3μm. This is roughly a factor of five below the 1 mm TCP requirement and a factor of seven below the 20μm pin target. This indicates that the mechanical performance is robust enough to tolerate the non-mechanical disturbance discussed in Section 7.2. The machined prototype cost 1880 USD, which is high for a single unit. The measured performance leaves significant margin in the contact-surface tolerances, so the cost can likely be reduced through relaxed tolerances and a more manufacturable redesign without losing the required precision. Overall, the prototype meets the criteria for the next step of industrial development.

Closing Remarks & Future Work. The mechanical fixture developed in this thesis reached a level of repeatability comparable in order of magnitude to the pin-level accuracy reported for laser-based joint offset calibration methods, but without optical hardware, calibration routines, or firmware modifications. The work targeted a narrower problem than full kinematic calibration, namely re-establishing joint zero quickly and cheaply after a joint is replaced. This is a problem that has received less attention in the literature than full calibration, and the results suggest that a passive mechanical solution is a practical way to address it. Future work on the project should focus on validating the concept across the full product range and verify the resulting TCP accuracy experimentally on a complete robot using external metrology systems. Long term durability testing for wear and thermal variation would improve the concept before industrial deployment. Improvements to ergonomics and fixture handling would further increase usability in a production environment.

Bibliography

Craig, J. J. (2005). *Introduction to Robotics: Mechanics and Control*. 3rd ed. Pearson Prentice Hall.

Elatta, A., L. P. Gen, F. L. Zhi, Y. Daoyuan, and L. Fei (2004). "An overview of robot calibration". *Information Technology Journal* **3**:1, pp. 74–78.

Gao, B., Y. Liu, N. Xi, and Y. Shen (2014). "Developing an efficient calibration system for joint offset of industrial robots". *Journal of Applied Mathematics* **2014**, p. 769343. DOI: 10.1155/2014/769343.

Kana, S., J. Gurnani, V. Ramanathan, S. H. Turlapati, M. Z. Ariffin, and D. Campolo (2022). "Fast kinematic re-calibration for industrial robot arms". *Sensors* **22**:6, p. 2295.

Liu, Y. and N. Xi (2011). "Low-cost and automated calibration method for joint offset of industrial robot using single-point constraint". *Industrial Robot: the international journal of robotics research and application* **38**:6, pp. 577–584. ISSN: 0143-991X. DOI: 10.1108/01439911111179093. eprint: https://www.emerald.com/ir/article-pdf/38/6/577/1190208/01439911111179093.pdf. URL: https://doi.org/10.1108/01439911111179093.

Mooring, B. W., Z. S. Roth, and M. R. Driels (1991). "Fundamentals of manipulator calibration".

Petrič, T. and L. Žlajpah (2023). "Kinematic model calibration of a collaborative redundant robot using a closed kinematic chain". *Scientific Reports* **13**, p. 17804. DOI: 10.1038/s41598-023-44929-9.

Toquica, J. S. and J. M. S. Motta (2022). "A methodology for industrial robot calibration based on measurement sub-regions". *The International Journal of Advanced Manufacturing Technology* **119**:1, pp. 1199–1216.

Wu, L., X. Zang, G. Ding, C. Wang, X. Zhang, Y. Liu, and J. Zhao (2023). "Joint calibration method for robot measurement systems". *Sensors* **23**:17, p. 7447.

Lund University
Department of Automatic Control
Box 118
SE-221 00 Lund Sweden

Document name
MASTER'S THESIS

Date of issue
June 2026

Document Number
TFRT-6311

Author(s)
Dante Neckmar

Supervisor
Nicholas Jones, Kassow Robots ApS, Denmark
Yiannis Karayiannidis, Dept. of Automatic Control, Lund University, Sweden
Bo Bernhardsson, Dept. of Automatic Control, Lund University, Sweden (examiner)

Title and subtitle
Improved Joint Zero Offset Calibration for Industrial Cobot Arms

Abstract

Collaborative robots, or cobots, are increasingly used in industrial automation, where they work in flexible, semi-modular configurations while still being expected to meet demanding positioning accuracy requirements. After a joint is replaced on such a robot, the resulting joint zero offset typically forces a full kinematic recalibration before the robot can return to service, causing downtime and requiring specialized equipment. Existing solutions are either simple manual references that lack the accuracy needed, or external optical systems that are expensive and complex to set up. This thesis develops a low-complexity, joint-level zeroing method for the cobot arms produced by Kassow Robots, with the goal of avoiding that recalibration step.

A sensitivity analysis showed that a pin-level repeatability of around 20µm is sufficient to keep the tool center point (TCP) positioning error below 1 mm across the full product range. Three concepts were considered: a mechanical fixture, a laser triangulation system, and a vision-based solution. The mechanical concept was chosen for its lower complexity and cost, and was designed and built as a cupshaped fixture with a self-locking block that engages the joint output through welldefined contact.

A 3D-printed prototype was used to validate the principle, and a machined stainless steel version was then tested over 96 zeroing cycles. The proposed prototype achieved a TCP standard deviation of 0.18 mm and a joint reference pin-level repeatability of about 3µm, well within the requirement. The results show that a passive mechanical fixture can deliver the precision needed for joint replacement without optical hardware or firmware modifications, removing the need for full kinematic recalibration after joint maintenance.

Keywords

Classification system and/or index terms (if any)

Supplementary bibliographical information

ISSN and key title
0280-5316

ISBN

Language
English

Number of pages
1-44

Recipient's notes

Security classification

http://www.control.lth.se/publications/